THE ASTRONOMICAL JOURNAL, 118:591–599, 1999 July

5145 PHOLUS STELLAR OCCULTATION CANDIDATES: 1999–2005

R. C. STONE
US Naval Observatory, Flagstaff Station, P.O. Box 1149, Flagstaff, AZ 86002; rcs@nofs.navy.mil
S. W. MCDONALD
Department of Earth, Atmospheric, and Planetary Sciences, Massachusetts Institute of Technology, Cambridge, MA 02139; mcdonald@astron.mit.edu
AND
J. L. ELLIOT
Department of Earth, Atmospheric, and Planetary Sciences and Department of Physics, Massachusetts Institute of Technology, Cambridge, MA 02139; and Lowell Observatory, Flagstaff, AZ 86001; jim@astron.mit.edu
Received 1999 February 9; accepted 1999 March 30

ABSTRACT

In search of stellar occultation candidates, the Flagstaff Automatic Scanning Transit Telescope (FASTT) was used to scan the sky through which the Centaur 5145 Pholus will pass during the period 1999–2005. Positions for 98,602 stars ($7.0 < V < 17.7$) were determined using differential reductions and the ACT catalog of star positions and proper motions, and accuracies of ± 20 mas in each coordinate were achieved, except for the faintest stars observed. During the period of our search, Pholus passes within 1.″5 of 100 of these stars, which have been identified as occultation candidates in this paper. Circumstances for the possible occultations are given, including finder charts for the 15 brightest stars. Since the radius of Pholus subtends approximately 10 mas, considerable astrometric effort will be required near the time of a potential event to determine whether it will result in an observable occultation. A stellar occultation observed from multiple sites can be used to determine the precise radius and albedo for this object.

Key words: astrometry — occultations

1. INTRODUCTION

This is next in a series of papers presenting stellar occultation candidates for interesting objects, which in the past have included Triton (McDonald & Elliot 1995), Pluto/Charon (McDonald & Elliot 1996), and 2060 Chiron (Person et al. 1996). This last object is a Centaur asteroid that has received considerable attention, since it is believed to be a Kuiper belt object (KBO) that has been perturbed into the inner solar system and is now exhibiting jetlike outbursts (Luu & Jewitt 1990; Meech & Belton 1990). There is a lot of interest in studying KBOs, but unfortunately they are so distant that, even with large-aperture telescopes, only limited photometric and spectroscopic information about them can be obtained. As a result, the Centaur asteroids, being much closer and accordingly brighter, offer perhaps the best means for studying the properties of their assumed KBO progenitors.

If the Centaurs are truly KBOs, then successfully observed occultations by them can provide important information about their physical sizes, albedos, and atmospheres. For example, Elliot et al. (1995) and Bus et al. (1996) observed occultations by Chiron in 1993 and 1994, finding absorption signatures of jets emitting from the nucleus and an extended coma. However, only a single nuclear chord was obtained. This allowed only a lower limit for its radius to be established from the occultation data, which is consistent with the radius obtained from modeling thermal data (Campins et al. 1994; Bus et al. 1996). Only Chiron, among the Centaurs, has been studied with an occultation. This paper provides occultation star candidates for another important Centaur, 5145 Pholus, and, hopefully, occultations of this interesting object can be observed as well. Pholus was discovered in 1992 and most likely is a KBO recently perturbed into the inner solar system. It is quite different from Chiron in that it is one of the reddest objects known in the solar system (Weintraub, Tegler, & Romanishin 1997), and according to Binzel (1992) and Wilson, Sagan, & Thompson (1994), its surface is probably coated with hydrocarbon ices, representative of the early formation of the solar nebula. Moreover, Hoffmann et al. (1993) argue that Pholus could be a bridge between comets and asteroids, inasmuch as it possesses characteristics of both classes of object. Its current orbit is eccentric ($e = 0.572$) and extends out to the orbit of Neptune (aphelion = 31.9 AU). But numerical integrations by Asher & Steel (1993) indicate that its orbit is unstable, and in $\sim 10^6$ yr Pholus could be ejected from the solar system after a close encounter with a major planet or, alternately, become a short-period comet (Levison & Duncan 1997).

However, predicting occultations for Pholus is challenging. Because of its current small angular size (radius ~ 10 mas), both its orbit and the position of any potential occultation star will have to be known extremely well in order to isolate the shadow path of Pholus across Earth at the time of the event. Fortunately, the means now exist for greatly improving the astrometry of asteroids and background stars by using the Tycho Catalogue (Høg 1997) of accurate star positions (about ± 25 mas in both coordinates) that can be augmented with good proper motions (i.e., the ACT Reference Catalog, described by Urban, Corbin, & Wycoff 1998). Moreover, these positions are in the International Celestial Reference Frame (ICRF), discussed by Ma et al. (1998), which is a quasi-inertial coordinate system defined at J2000 that has been adopted by IAU resolution to be the standard for all future astrometric reductions. This paper presents results determined from measuring accurate ICRF/J2000 positions for 98,602 stars along the path of Pholus in the years 1998.5 to 2006.0 in order to search for occultation candidates.

Section 2 describes the CCD observations and their reduction to equatorial coordinates for the stars considered in this paper; § 3 gives a list of possible stars that might be occulted by Pholus in 1999–2005, along with finder charts for some of the brightest stars; in § 4, the conclusions of this paper are summarized.

2. OBSERVATIONS AND REDUCTIONS

All of the observations were taken with the Flagstaff Astrometric Scanning Transit Telescope (FASTT), which is an automated 20 cm meridian telescope (scale = 99″ mm^{-1}) equipped with a thick front-illuminated Ford/Loral 2048^2 CCD with 15 μm pixels. The field of view is 50′.7 × 50′.7, and the light is filtered with a *Hubble Space Telescope* F606W (4700–7300 Å) broadband filter. All observations were taken in scan mode, wherein the telescope is kept stationary, and the charge images of stars are clocked at the diurnal rate in order to prevent smearing. As discussed in Stone et al. (1996), scan observing can be done in several ways, including clocking the image of each star across the entire width of the CCD (full scanning) or only across part of the CCD followed with a rapid readout of the chip after the shutter is closed (partial scanning). The main advantage of the latter method is that short exposures can be chosen, but as a consequence, some of the CCD pixel area is taken up by either the ramp-up or ramp-down of the scan exposure. This causes the useful area of the CCD scan to be foreshortened in right ascension by an amount equal to the chosen exposure time. Unfortunately, FASTT can observe only in scan mode, since the telescope cannot be driven in right ascension, and full scanning causes all but the very faintest ACT reference stars (Urban et al. 1998) to be saturated and herein considered unmeasurable. Consequently, all the observations presented in this paper were taken while partial-scanning with an adopted exposure time of 50 s, yielding a useful magnitude range of $9.0 < V < 17.7$. In some cases, a shorter exposure of 10 s was used to extend the bright magnitude limit to $V = 7.0$.

The observing strategy is illustrated in Figure 1, where partial-scanning boxes (herein defined as 50 s FASTT scan exposures that yield a useful CCD area of 38′.2 × 50′.7) were observed along the path of 5145 Pholus in 1998.5 to 2006.0. The scan boxes overlap by 5% or more and cover a swath ∼51′ wide along the path of the asteroid during this time period. Each scan box was observed twice, the box centers were shifted by $\frac{1}{2}$ box width, and then more observations were taken. This method of observation was chosen to reduce systematic errors in star positions caused by their placement on the CCD during an exposure, and each star was observed typically four times. A total area of 88 deg^2 was scanned for star positions, and Table 1 gives more details about the FASTT observations.

The processing for star positions consisted of several stages. At first, all measurable stars were identified with a local-maxima search and centered with a Gaussian fit (see Stone et al. 1996 for more details). Neither saturated stars nor those with badly elongated images (i.e., those having axial ratios exceeding 2) were included. Next, the ACT reference stars in each scan box were matched with their corresponding FASTT (x, y) pixel positions, and standard coordinates (X, Y) were computed for them using the routines given by Green (1985, p. 310). The FASTT pixel and ACT standard coordinates were related then with the following linear transformations, allowing for zero-point, orientation, and scale changes:

$$x - X = c_1 + c_2 x + c_3 y , \quad (1)$$

$$y - Y = c'_1 + c'_2 x + c'_3 y , \quad (2)$$

where (c, c') are coefficients solved for with least squares. All of the scan boxes were processed in this manner, and an analysis of FASTT-minus-ACT residuals produced by these fits showed no systematic trends when plotted against x- and y-coordinate positions, as well as magnitude. Hence, the linear model chosen for the astrometric reductions seemed appropriate. Equations (1) and (2) were used to transform all the FASTT (x, y) pixel positions to standard coordinates, which, in turn, were converted to ICRF/J2000 equatorial coordinates using other routines given by Green (1985, p. 310). The ACT reference stars gave excellent results, since the least-squares fit errors were typically ±50 mas in each coordinate. Finally, the equatorial positions for each FASTT star were collated, and mean positions and their formal errors were formed. In all, positions were determined for 98,602 stars brighter than $V \sim 17.7$. These are summarized in Table 2 and shown in Figure 2. The last

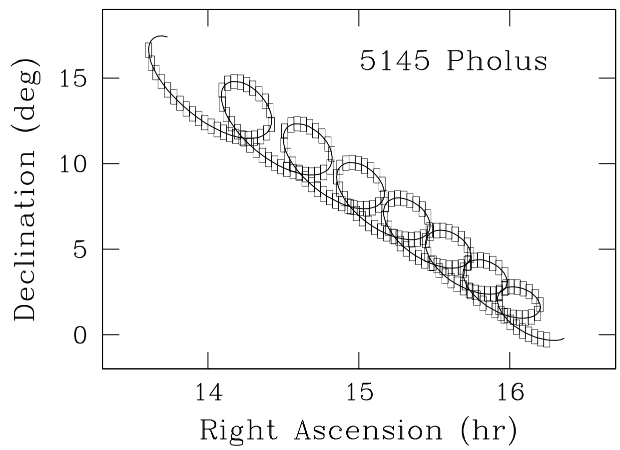

FIG. 1.—Orbital path of 5145 Pholus in 1998.5 to 2006.0, shown along with overlapping FASTT scan boxes used to identify stars that might be occulted by the asteroid. Each box is 38′.2 × 50′.7 in size. The boxes shown in the diagram were each scanned twice, and then the process was repeated with a second set of boxes, whose centers were shifted by 50% relative to the first set. In all, each star was observed about four times.

TABLE 1

CHARACTERISTICS OF THE STAR OBSERVATIONS

Characteristic	Value
5145 Pholus orbital time coverage	1998.5–2006.0
CCD scan frames taken	820
Exposure	50 s
Stars surveyed	98,602
CCD images per star	3.94
Mean epoch of observation	1998.35
Range in R.A. (ICRF/J2000)	13^{h}34^m.9 to 16^{h}18^m.3
Range in decl. (ICRF/J2000)	−0°45′ to 17°3′
Total area scanned	88 deg^2
Central Galactic coordinates (l, b)	(6°.5, 54°.2)
Range in V magnitude	7.0–17.7
Magnitude completeness	$V \lesssim 17.1$

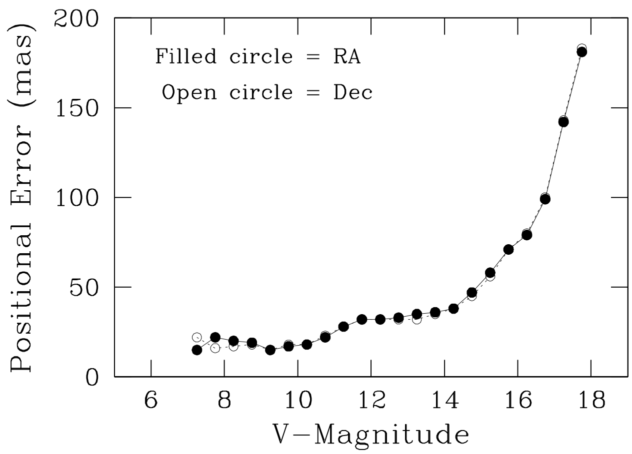

FIG. 2.—Accuracy of FASTT star positions in both right ascension and declination as a function of visual magnitude. The FASTT positions are quite accurate (±50 mas or better), except for the faintest stars observed.

column of the table gives the number of FASTT stars observed in each interval of magnitude.

As seen, the accuracies are about ±20 mas in both coordinates for the brighter stars, which degrade, because of low count rates, to about ±180 mas for the faintest stars observed. As discussed above, these are internal errors. The true accuracy of FASTT star positions can be determined by comparing them externally with objects with extremely well known positions. For example, Figures 3 and 4 show (FASTT − ACT) differences in position plotted against equatorial coordinates and visual magnitude. There are 828 stars in common, and neither diagram shows evidence for systematic trends. Moreover, the dispersions in these differences are, respectively, ±40 mas in both coordinates, when only the ACT stars ($V < 9.5$) with the best accuracies are included (Høg 1997). These dispersions can be explained by

TABLE 2

MEAN ACCURACY OF THE FASTT STAR POSITIONS AND MAGNITUDES

V	σ(R.A.) cos δ (mas)	σ(decl.) (mas)	$\sigma(V)$ (mag)	Number of Stars
7.0–7.5	15	22	0.005	7
7.5–8.0	22	16	0.009	9
8.0–8.5	20	17	0.006	14
8.5–9.0	19	18	0.024	63
9.0–9.5	15	15	0.022	106
9.5–10.0	17	18	0.022	182
10.0–10.5	18	18	0.021	270
10.5–11.0	22	23	0.024	397
11.0–11.5	28	28	0.021	556
11.5–12.0	32	32	0.023	820
12.0–12.5	32	32	0.022	1148
12.5–13.0	33	32	0.022	1745
13.0–13.5	35	32	0.023	2211
13.5–14.0	36	35	0.024	3246
14.0–14.5	38	38	0.025	4432
14.5–15.0	47	45	0.029	6067
15.0–15.5	58	56	0.035	8105
15.5–16.0	71	71	0.042	10964
16.0–16.5	79	80	0.047	13594
16.5–17.0	99	100	0.057	16916
17.0–17.5	142	143	0.079	20031
17.5–18.0	181	183	0.100	7719

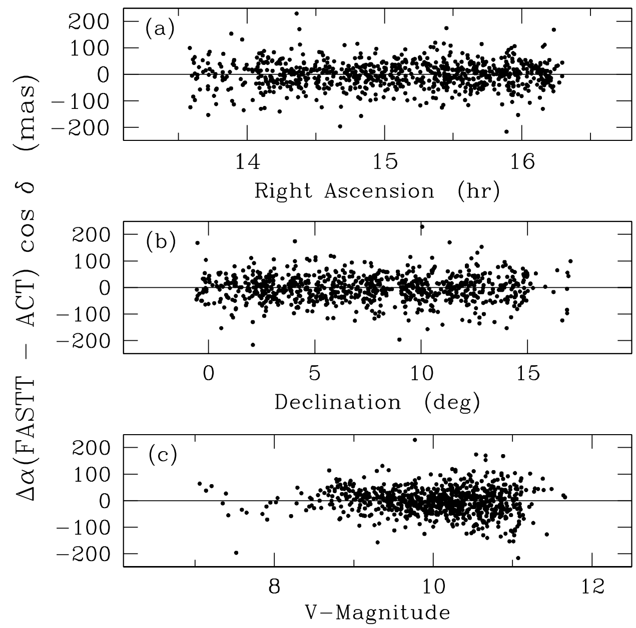

FIG. 3.—Differences between FASTT and ACT catalog right ascensions plotted against (*a*) right ascension, (*b*) declination, and (*c*) magnitude. There is no evidence of systematic trends in any of the plots, and the scatter can be explained by FASTT observational and known ACT catalog errors (see text for more details).

FASTT observational and quoted ACT catalog errors, when added in quadrature. In both coordinates, the expected dispersion is ±38 mas, which is in excellent agreement with the dispersion quoted above. Hence, the errors quoted in Table 2 are realistic at least for the brighter stars ($V < 11.5$). For fainter stars, another method of evaluation was used. Namely, FASTT also observed a number of faint radio reference objects, taken from Johnston et al. (1995),

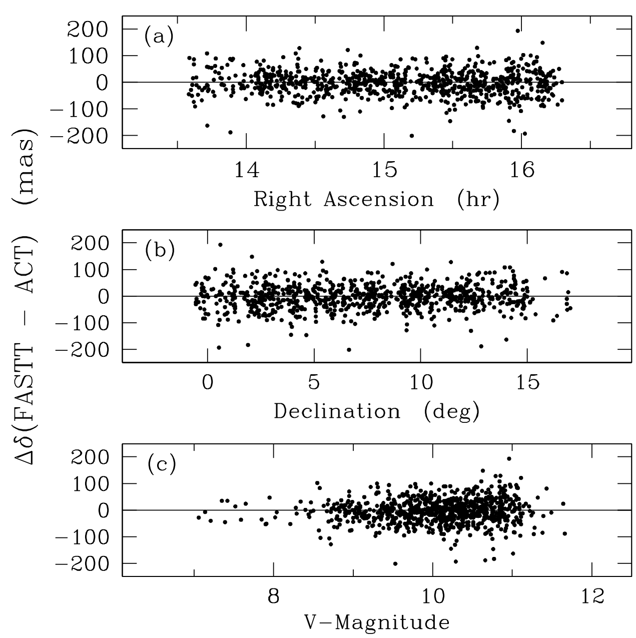

FIG. 4.—Similar to Fig. 3, but showing (FASTT − ACT) differences in declination plotted against equatorial coordinates and magnitude. Again, there is no evidence of systematics in the FASTT star positions, and the scatter in declination can be explained by FASTT observational and ACT catalog errors.

whose positions are known to ± 1 mas or better. In all, nine radio reference sources were observed repeatedly, and the differences in positions were found to be $\Delta\alpha$(FASTT $-$ radio) $\cos\delta = -14$ mas and $\Delta\delta$(FASTT $-$ radio) $= -2$ mas over the magnitude interval $15.3 < V < 17.5$. Both results indicate that the FASTT positions for faint stars are systematically well determined, and the scatter in these measurements indicate also that the observational errors quoted in Table 2 are realistic. Nonetheless, the accuracy of FASTT star positions will degrade in time (away from their mean epochs of observation, $\sim$1998.35), because proper motions are only known of a small number of them. The expected rate of degradation is $\sim$14 mas yr^{-1}.

Moreover, accurate magnitudes were determined for each of the FASTT stars using aperture photometry. An aperture of 12″, centered on each star, was chosen with the local sky background determined in a surrounding concentric annulus with inner and outer radii of 18″ and 30″, respectively. Flattening was achieved by illuminating a flat screen inside the telescope enclosure. Count rates (DN s^{-1}) were then computed for each star by correcting the aperture reading for the contribution made by the sky (see Henden & Stone 1998 for more details). Next these count rates, CR, were converted to visual magnitudes with the following standard photometric relation:

$$V = \zeta - k_1 X - 2.5 \log \mathrm{CR} + \epsilon_v (B-V) , \quad (3)$$

where ζ is a zero-point correction, k_1 is the primary extinction coefficient, X is the air mass at the time of the observation, and ϵ_v is the instrumental color coefficient, which is known to be $\epsilon_v = 0.363 \pm 0.003$ (s.e.) from observations of Landolt standard fields. Photometric (B, V) standards in each FASTT scan box were taken from the Tycho Catalogue (Høg 1997), matched with their corresponding FASTT count rates, and then used to compute the ζ and k_1 coefficients in equation (3) with least squares. Once established, these coefficients and the equation were used to convert all of the stellar count rates in each scan box to visual magnitudes. In general, only the Tycho standards present in each scan box have $B-V$ colors known for them. For the other stars, a color of $B-V = 0.7$ mag, typical of faint stars at a similar Galactic latitude, was assumed and used in equation (3) to compute their magnitudes. Hence, each of their magnitudes is affected by a color term amounting to $\Delta V = \epsilon_v [(B-V) - 0.7]$, where $B-V$ is the true stellar color. Based on known photometry of faint stars, the color terms should be $|\Delta V| < 0.15$ mag in most cases, and this uncertainty can be eliminated if good $B-V$ colors should eventually become available for these stars. Table 2 gives the internal accuracy (mean error of the mean) of the FASTT magnitudes as a function of magnitude, and as seen, it ranges from ± 0.01 mag for the brighter stars to ± 0.10 mag for the faintest.

3. RESULTS AND DISCUSSION

We identified stellar occultation candidates for 5145 Pholus with an ephemeris integrated from the database of asteroids maintained[1] by E. Bowell and L. H. Wasserman at Lowell Observatory (the 1998 September 8 version). The list of objects identified by FASTT was then culled to find those with $V = 18.0$ or brighter that lay within 1″.5 of the ephemeris. No bodies were excluded by our usual criterion for a minimum solar elongation of 20° (McDonald & Elliot 1995, 1996), because the minimum distance between Pholus and the Sun never goes below 21° during our search interval.

The candidates are listed in Table 3. The first column gives an identification label beginning with "Ph" and followed by a sequence number. The next columns show the date and time of Pholus's closest approach to the star and the minimum separation and position angle of Pholus from the star (measured north through east) at that time for a geocentric observer. An estimated V magnitude of the star (as discussed in the previous section) is in the next column, followed by the velocity of the occultation shadow in the fundamental plane (Smart 1977). The next column is the angular distance of the star from the Sun. The observed J2000 coordinates of the star in the ICRF reference frame come next, followed by the east longitude of the substellar point at event time. The last two columns are the distance between Pholus and Earth and the estimated V magnitude of Pholus. These latter two columns have been added to our usual format because Pholus is rapidly receding from the Sun. During its 1998 opposition (1998 March 31), Pholus was 12.128 AU from Earth and had an apparent magnitude of $V = 18.2$. By the time of the opposition in 2005 (2005 May 12), Pholus will be 18.646 AU from Earth and will have dimmed to $V = 20.0$.

Two objects were rejected from the list of occultation candidates because they were clearly nonstellar and most likely galaxies. Four other objects appear to be slightly fuzzy or extended but have been retained in the candidate list: Ph7, Ph32, Ph38, and Ph71. Before planning to observe a Pholus occultation of any of these four objects, observers should very carefully examine the object to determine whether it is an extended source. Occultations of extended sources produce poor data at best; the analysis is greatly complicated by trying to model the extended source, and the depth of the occultation is greatly reduced. All of the other objects in the candidate list appear stellar in their CCD images and on the Digitized Sky Survey (DSS).

Our limiting separation of 1″.5 between the Pholus ephemeris and a potential candidate allows for (1) the parallax of 1 Earth radius and (2) potential sources of error in these predictions. The main sources of error are inaccuracies in the measured positions of the stars, the effects of their unknown proper motions, and error in the Pholus ephemeris. The accuracy the stellar positions and the effects of proper motion are discussed in § 2. The dominant source of error is caused by uncertainties in the ephemeris for Pholus. Although the best available positions were used in its creation, many of these contain large errors, because of the systematic errors present in the star catalogs used to reduce them. For example, many were reduced differentially with respect to the Guide Star Catalog, which is known to have systematic errors that can exceed $\pm$0″.5 in each coordinate. Accordingly, the times of events and minimum separations given in Table 3 are subject to change, although the identification of occultation candidates will remain the same. The uncertainties in the ephemeris used in this study will generally increase over time and could approach 0″.5 by the end of the period of study. Proper-motion and ephemeris error increase with time, and the parallax of an Earth radius will decrease from 0″.73 for the 1998 opposition to 0″.47 for the 2005 opposition. New observations of Pholus

[1] At World Wide Web site ftp://ftp.lowell.edu/pub/elgb/astorb.html.

TABLE 3

Possible Occultations by 5145 Pholus in 1999–2005

Star ID	Event Date	UT	Minimum Separation (arcsec)	Position Angle (deg)	Star Mag. (V)	Shadow Velocity (km s^{-1})	Solar Angle (deg)	R.A. (J2000)	Decl. (J2000)	East Long. (deg)	Dist. to Pholus (AU)	Pholus Mag. (V)
Ph1	1998 Aug 29	2358	0.43	216	16.0	31.3	47	13 44 18.769	+14 14 23.74	−132	14.092982	18.7
Ph2	1998 Sep 14	1639	1.22	210	15.9	34.9	36	13 48 31.066	+13 34 48.89	−36	14.269962	18.7
Ph3	1998 Oct 2	2352	0.62	205	15.4	37.4	26	13 54 06.526	+12 52 22.66	−161	14.410810	18.7
Ph4	1998 Oct 5	0500	0.77	204	17.6	37.6	25	13 54 49.229	+12 47 38.60	120	14.422634	18.7
Ph5	1998 Oct 23	0435	1.04	199	16.9	37.8	24	14 00 45.567	+12 13 13.04	110	14.475217	18.7
Ph6	1998 Oct 31	0530	0.52	17	15.8	37.2	26	14 03 26.737	+12 00 30.52	89	14.473344	18.7
Ph7[a]	1998 Dec 1	1633	0.77	186	17.5	31.0	47	14 13 26.279	+11 30 28.36	−105	14.324093	18.8
Ph8	1998 Dec 15	1139	0.12	179	16.5	26.8	59	14 17 13.169	+11 28 15.12	−45	14.197151	18.8
Ph9	1999 Jan 25	0213	0.44	312	12.8	13.6	95	14 24 27.874	+12 01 05.43	59	13.704183	18.8
Ph10 ...	1999 Mar 3	0650	0.42	58	16.4	15.9	128	14 24 30.819	+13 08 38.24	−47	13.286736	18.7
Ph11 ...	1999 May 14	2338	0.34	184	11.7	19.1	142	14 11 26.440	+14 47 48.62	−14	13.304280	18.6
Ph12 ...	1999 Sep 4	0611	1.23	217	17.9	30.1	50	14 11 41.681	+11 52 05.32	137	15.044447	19.0
Ph13 ...	1999 Sep 10	2311	1.22	34	14.6	31.9	45	14 13 12.753	+11 36 13.24	−124	15.129925	19.0
Ph14 ...	1999 Oct 18	2320	0.23	21	17.1	37.4	24	14 23 41.627	+10 16 18.07	−161	15.437499	19.0
Ph15 ...	1999 Oct 28	0449	0.67	19	17.1	37.4	23	14 26 31.000	+10 00 57.03	108	15.461122	19.0
Ph16 ...	1999 Nov 18	1858	1.23	12	16.8	35.2	33	14 33 07.452	+09 33 47.25	−124	15.435256	19.0
Ph17 ...	1999 Dec 8	1410	0.56	184	15.8	30.7	47	14 38 46.729	+09 21 21.55	−70	15.317987	19.1
Ph18 ...	1999 Dec 8	1538	0.89	4	14.9	30.6	47	14 38 47.702	+09 21 18.99	−92	15.317501	19.1
Ph19 ...	2000 Feb 24	1606	0.54	256	11.9	13.1	116	14 49 17.340	+10 30 08.28	−173	14.411012	19.0
Ph20 ...	2000 Mar 29	1018	1.16	215	14.3	20.2	144	14 45 59.098	+11 29 40.31	−120	14.143462	18.9
Ph21 ...	2000 Jul 8	0814	1.18	289	15.1	12.1	103	14 30 01.842	+11 42 51.16	167	14.962638	19.1
Ph22 ...	2000 Sep 2	1357	0.99	220	15.9	27.5	56	14 34 13.395	+09 51 29.43	27	15.914684	19.3
Ph23 ...	2000 Sep 21	1456	1.43	211	17.6	32.6	41	14 38 07.703	+09 10 30.04	−5	16.162941	19.3
Ph24 ...	2000 Oct 14	1650	0.22	24	15.9	36.4	27	14 43 58.767	+08 25 35.83	−55	16.366042	19.2
Ph25 ...	2000 Nov 10	0516	0.72	15	16.3	36.6	25	14 51 28.404	+07 46 06.34	94	16.442878	19.2
Ph26 ...	2000 Nov 13	2152	1.19	14	17.6	36.2	27	14 52 31.744	+07 41 55.70	−158	16.439787	19.3
Ph27 ...	2000 Dec 7	1735	0.25	6	14.4	31.9	42	14 59 04.568	+07 24 12.46	−116	16.341944	19.3
Ph28 ...	2000 Dec 24	0420	1.14	358	16.3	26.9	55	15 03 03.302	+07 21 49.11	67	16.204755	19.3
Ph29 ...	2001 Jan 24	2111	0.36	330	17.2	15.8	83	15 08 31.159	+07 39 54.93	145	15.833457	19.3
Ph30 ...	2001 Feb 26	1511	1.06	78	14.6	12.4	113	15 10 04.565	+08 23 19.79	−157	15.420171	19.2
Ph31 ...	2001 Jun 9	0949	0.82	169	17.1	17.6	133	14 54 46.415	+10 01 16.85	178	15.387828	19.3
Ph32[a]...	2001 Jun 17	2218	0.57	160	17.3	15.8	126	14 53 34.634	+09 56 27.59	−18	15.499543	19.3
Ph33 ...	2001 Sep 6	0259	0.77	221	17.5	26.2	58	14 54 42.970	+07 50 02.80	−167	16.834265	19.5
Ph34 ...	2001 Oct 10	1516	0.01	196	16.1	34.5	32	15 01 44.504	+06 44 07.06	−23	17.250696	19.5
Ph35 ...	2001 Oct 12	0756	0.33	25	17.5	35.0	31	15 02 09.160	+06 41 11.44	85	17.264854	19.5
Ph36 ...	2001 Oct 14	0107	0.19	25	17.7	35.3	30	15 02 34.474	+06 38 16.31	−174	17.278555	19.5
Ph37 ...	2001 Nov 4	0014	0.15	20	15.7	36.5	23	15 07 59.984	+06 06 47.47	180	17.387854	19.5
Ph38[a]...	2001 Nov 11	0160	0.05	196	17.5	36.6	23	15 09 53.708	+05 58 11.12	147	17.399971	19.5
Ph39 ...	2001 Dec 14	1514	0.67	184	13.7	30.9	43	15 18 34.978	+05 34 16.90	−83	17.290384	19.6
Ph40 ...	2002 Jan 11	1049	1.04	169	12.0	22.1	66	15 24 20.574	+05 37 42.55	−42	17.023605	19.6
Ph41 ...	2002 Feb 3	2237	0.12	141	17.3	13.9	87	15 27 22.158	+05 56 08.19	118	16.727136	19.6
Ph42 ...	2002 Mar 15	1907	0.54	234	16.9	14.7	123	15 27 38.091	+06 48 42.68	132	16.242959	19.5
Ph43 ...	2002 Mar 21	0110	1.20	47	14.4	16.1	128	15 27 12.670	+06 56 20.86	36	16.193266	19.5
Ph44 ...	2002 Mar 30	1015	1.04	38	17.2	18.3	136	15 26 13.561	+07 09 43.79	−110	16.117777	19.4
Ph45 ...	2002 Jun 6	1940	0.82	355	17.2	19.9	140	15 14 36.143	+07 59 12.05	38	16.230129	19.5
Ph46 ...	2002 Jun 12	0627	0.46	172	16.2	18.9	136	15 13 44.699	+07 57 41.35	−129	16.290354	19.5
Ph47 ...	2002 Jul 10	0346	0.35	313	16.5	12.9	113	15 10 33.556	+07 36 34.11	−117	16.685858	19.6
Ph48 ...	2002 Jul 23	1530	0.12	283	14.9	12.4	101	15 09 54.548	+07 19 27.80	53	16.913720	19.6
Ph49 ...	2002 Aug 5	2038	1.08	257	17.4	14.3	90	15 09 54.531	+06 59 24.71	−37	17.147164	19.7
Ph50 ...	2002 Oct 17	2059	0.17	24	15.8	34.7	31	15 20 11.827	+04 51 47.71	−111	18.200138	19.7
Ph51 ...	2002 Oct 20	1035	1.02	203	16.7	34.7	29	15 20 47.712	+04 47 55.50	43	18.220212	19.7
Ph52 ...	2002 Oct 23	1925	0.48	22	15.8	35.5	28	15 21 35.540	+04 42 57.03	−93	18.244179	19.7
Ph53 ...	2002 Dec 27	1744	0.73	360	16.2	28.5	49	15 37 17.836	+03 53 26.85	−128	18.156481	19.8
Ph54 ...	2003 Jan 14	1814	0.01	165	17.4	22.3	65	15 40 38.423	+03 57 53.96	−152	17.970867	19.8
Ph55 ...	2003 Jan 18	1535	0.89	166	15.3	20.5	68	15 41 14.630	+03 59 53.73	−116	17.924900	19.8
Ph56 ...	2003 Jan 26	1136	0.15	339	15.4	17.9	75	15 42 18.931	+04 04 54.08	−64	17.827644	19.8
Ph57 ...	2003 Feb 18	1023	0.40	299	17.1	11.2	96	15 44 12.886	+04 26 31.73	−68	17.524866	19.8
Ph58 ...	2003 Apr 12	0918	0.15	28	15.6	20.2	142	15 41 15.844	+05 33 12.96	−104	16.983390	19.6
Ph59 ...	2003 Aug 23	0540	1.32	59	16.1	17.5	79	15 27 03.942	+04 49 21.12	175	18.271800	19.9
Ph60 ...	2003 Sep 3	0554	0.48	228	17.3	21.1	70	15 27 58.931	+04 31 11.92	161	18.460995	19.9
Ph61 ...	2003 Sep 16	0912	0.45	219	16.8	25.4	59	15 29 34.356	+04 09 08.04	99	18.671343	19.9
Ph62 ...	2003 Oct 18	0417	0.93	24	13.6	33.7	34	15 35 17.590	+03 18 41.30	143	19.066139	19.9
Ph63 ...	2003 Oct 25	0013	0.50	22	17.4	34.4	29	15 36 46.979	+03 09 10.44	−162	19.123416	19.9
Ph64 ...	2003 Dec 12	2247	0.04	184	16.6	33.2	34	15 48 17.356	+02 25 11.78	174	19.190371	20.0

TABLE 3—*Continued*

Star ID	Event Date	UT	Minimum Separation (arcsec)	Position Angle (deg)	Star Mag. (*V*)	Shadow Velocity (km s^{-1})	Solar Angle (deg)	R.A. (J2000)	Decl. (J2000)	East Long. (deg)	Dist. to Pholus (AU)	Pholus Mag. (*V*)
Ph65	2003 Dec 18	0430	0.64	5	16.7	32.1	38	15 49 27.689	+02 23 29.67	83	19.162162	20.0
Ph66	2003 Dec 19	1619	0.70	184	17.2	31.3	39	15 49 47.253	+02 23 09.55	−95	19.152899	20.0
Ph67	2004 Jan 19	0341	0.29	168	17.4	21.8	64	15 55 30.055	+02 26 57.75	65	18.869924	20.0
Ph68	2004 Feb 4	0246	1.48	153	11.8	15.8	79	15 57 30.436	+02 36 56.76	64	18.669586	20.0
Ph69	2004 Apr 10	1156	0.79	211	15.7	19.2	139	15 56 25.975	+03 49 03.00	−139	17.900436	19.9
Ph70	2004 Apr 23	1760	0.93	202	17.9	21.8	148	15 54 36.199	+04 02 23.77	116	17.831160	19.8
Ph71[a] ...	2004 Jun 3	1804	0.94	1	16.6	22.3	149	15 47 42.494	+04 23 05.37	73	17.910564	19.8
Ph72	2004 Aug 3	1649	0.19	100	17.3	12.2	100	15 41 28.147	+03 41 59.17	30	18.737396	20.1
Ph73	2004 Aug 7	2019	0.21	90	17.2	12.6	96	15 41 26.067	+03 36 37.49	−26	18.810533	20.1
Ph74	2004 Oct 6	1018	1.13	209	12.1	30.0	45	15 46 58.535	+02 08 00.02	67	19.776400	20.1
Ph75	2004 Nov 1	0924	0.26	199	16.7	35.0	26	15 52 08.170	+01 33 51.18	56	20.025459	20.1
Ph76	2004 Nov 7	0301	0.65	18	11.7	35.6	24	15 53 23.966	+01 27 29.70	146	20.058902	20.1
Ph77	2004 Nov 9	0800	0.18	17	17.2	35.7	23	15 53 53.504	+01 25 12.64	69	20.069426	20.1
Ph78	2004 Nov 10	0129	0.46	197	14.8	35.7	23	15 54 03.370	+01 24 28.53	166	20.072692	20.1
Ph79	2004 Nov 27	1420	0.17	11	16.9	35.4	23	15 58 03.364	+01 09 27.78	−43	20.108731	20.1
Ph80	2004 Nov 29	0328	0.65	11	16.1	35.3	23	15 58 24.431	+01 08 25.45	119	20.107909	20.1
Ph81	2004 Nov 29	1147	0.91	11	14.3	35.4	23	15 58 29.170	+01 08 11.54	−6	20.107682	20.1
Ph82	2004 Dec 19	1726	0.10	184	15.4	32.1	36	16 02 57.838	+00 59 13.31	−110	20.041225	20.2
Ph83	2004 Dec 29	2032	0.65	0	16.9	29.5	44	16 05 01.415	+00 57 58.38	−166	19.971614	20.2
Ph84	2005 Jan 10	1847	0.54	355	17.6	25.7	54	16 07 12.449	+00 59 17.96	−151	19.862899	20.2
Ph85	2005 Jan 29	0934	0.65	162	17.4	18.7	71	16 09 55.248	+01 07 07.43	−30	19.647629	20.2
Ph86	2005 Feb 16	0028	0.58	136	17.0	12.3	87	16 11 32.338	+01 20 02.51	90	19.413563	20.2
Ph87	2005 Feb 20	1113	0.35	309	16.5	11.2	91	16 11 47.066	+01 23 59.11	−76	19.352783	20.2
Ph88	2005 Jun 5	2316	0.34	1	15.8	23.2	151	16 01 24.878	+02 48 20.00	−3	18.742183	20.0
Ph89	2005 Jun 29	1720	1.10	165	15.1	18.4	134	15 57 56.766	+02 42 45.44	61	18.973701	20.1
Ph90	2005 Jul 6	1923	1.21	159	15.6	16.9	128	15 57 07.013	+02 38 41.37	23	19.066621	20.1
Ph91	2005 Jul 24	1214	1.29	312	11.5	12.8	113	15 55 37.268	+02 24 08.19	113	19.335608	20.2
Ph92	2005 Aug 25	1025	0.65	246	15.5	14.7	84	15 55 19.503	+01 46 06.70	108	19.892979	20.3
Ph93	2005 Sep 24	1427	0.73	36	15.7	24.5	58	15 57 58.513	+01 03 43.73	19	20.398983	20.3
Ph94	2005 Oct 12	1849	0.43	27	15.5	30.3	43	16 00 45.416	+00 38 58.06	−64	20.646891	20.3
Ph95	2005 Oct 14	0853	0.16	25	15.5	30.2	42	16 01 02.034	+00 36 55.29	84	20.665552	20.3
Ph96	2005 Oct 28	2311	0.46	201	17.2	33.4	31	16 03 47.453	+00 19 13.79	−144	20.811738	20.3
Ph97	2005 Nov 4	0814	0.67	18	16.1	34.6	27	16 05 05.403	+00 12 17.14	74	20.859754	20.3
Ph98	2005 Nov 26	1250	1.32	192	17.1	35.5	21	16 09 52.384	−00 07 03.92	−16	20.946204	20.3
Ph99	2005 Dec 12	1201	0.92	7	17.6	34.0	28	16 13 20.436	−00 15 43.97	−18	20.928365	20.3
Ph100...	2005 Dec 21	2358	0.62	4	15.7	32.2	34	16 15 19.109	−00 18 32.51	153	20.887017	20.3

NOTE.—Units of right ascension are hours, minutes, and seconds, and units of declination are degrees, arcminutes, and arcseconds.
[a] Possibly nonstellar.

are planned, which should dramatically improve the predictions presented in this paper.[2]

While it is not possible to say with certainty which of these candidates will be occulted by Pholus, some candidates are worthy of particular attention. Bright stars involved in occultation with low shadow-plane velocities will yield data with the best signal-to-noise ratio (S/N). The spatial resolution is determined by the S/N, shadow-plane velocity, integration time, and Fresnel scale. Numerous events in the candidate list have geocentric sky-plane velocities between 11 and 15 km s^{-1}. The brightest stars among the occultation candidates ($V < 13.0$), listed in order of increasing predicted minimum separation, are Ph11, Ph19, Ph76, Ph40, Ph91, and Ph68. Stars brighter than $V = 14.0$ mag and with low minimum separations are Ph9, Ph11, Ph27, Ph48, and Ph78. These five stars are the most likely to produce useful occultations, although Pholus is rather close to the Sun at the time of its closest approach to Ph78.

Figure 5 shows finder charts (extracted from the DSS) for all of the stars brighter than $V = 15.0$ with appulse events more than 40° from the Sun. This appears to be the practical limit for occultation observations with a portable 0.35 m telescope equipped with a CCD photometer (Bus et al. 1996). Finder charts for other occultation candidates may be created by observers using the DSS and the star coordinates in Table 3. Figure 6 depicts views of Earth from Pholus for each candidate in Figure 5 at the time of appulse. Each view is intended to give potential observers some idea of what parts of Earth might be able to see each occultation event. Many of the globes in Figure 6 include a set of lines indicating the nominal track and northern and southern limits of the shadow path. Tracks are shown only when they cross Earth.

Note that each nominal track is merely the result of using the current Pholus ephemeris and the corresponding star position listed in Table 3, and errors in both the star position and the Pholus ephemeris will affect both the event time and the minimum geocentric separation given in Table 3. Astrometric errors parallel to the track will affect the time at which the occultation occurs, while errors perpendicular

[2] Updates to the predictions presented in this paper will be given at the Web site occult.mit.edu, after these new data become available.

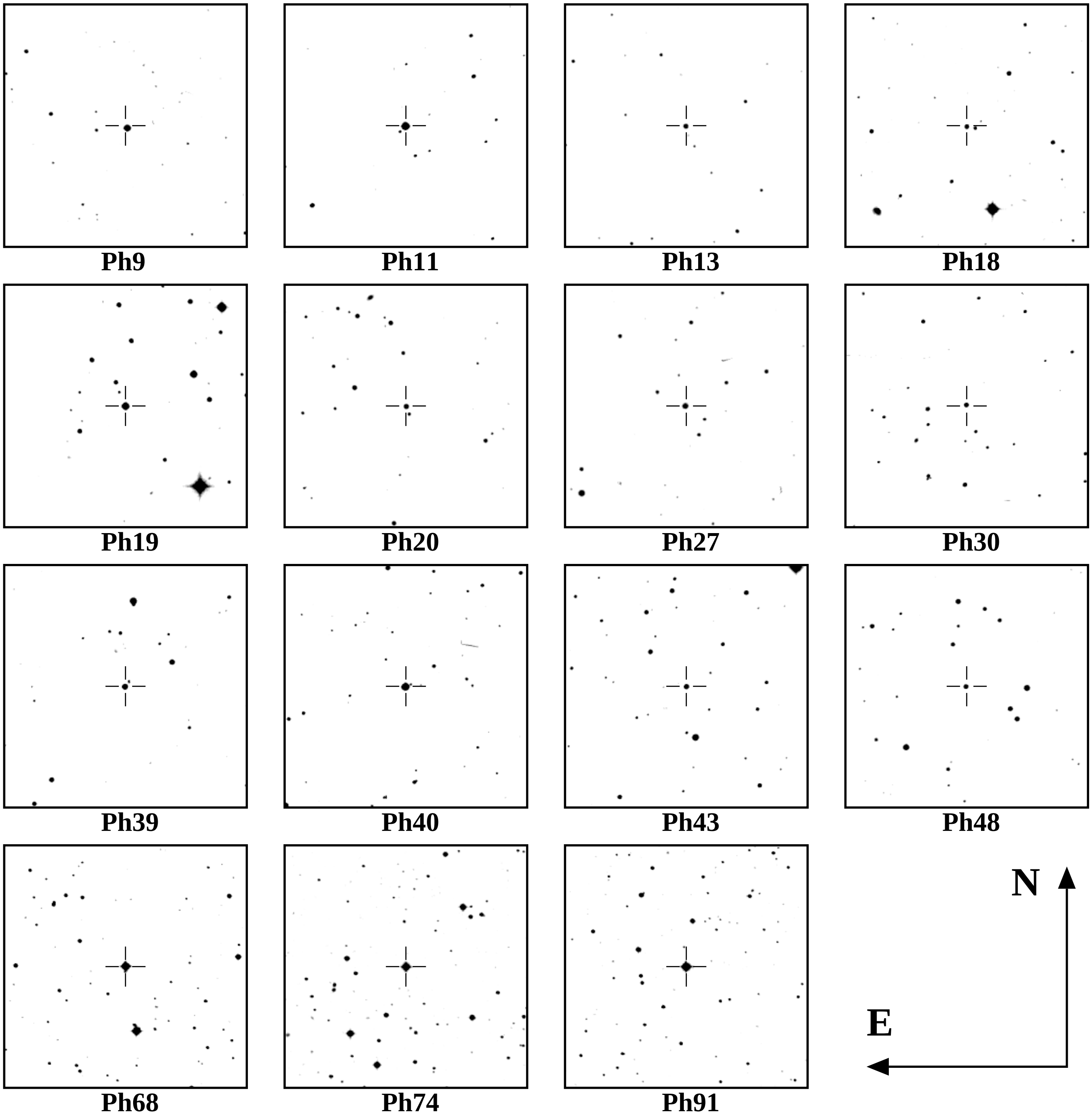

FIG. 5.—Finder charts for the brightest Pholus candidate occultation stars ($V < 15.0$) given in Table 3, excluding those closer than 40° to the Sun at appulse time. These charts were produced from the Digitized Sky Survey, and each box is 7′ on a side. The occultation star is marked at the center of each panel.

to the track will displace the position of the track either north or south of the nominal track, possibly by more than the apparent radius of Earth. As discussed above, these tracks are subject to considerable error because of uncertainties in the ephemeris for Pholus. Consequently, the tracks shown in Figure 6 are only intended to be suggestive.

The Pholus ephemeris is least accurate during the later years of this study. For this reason, further observations of the occultation candidates and Pholus are necessary to refine each occultation prediction. Given the small width of the occultation shadow, it will be difficult to refine Pholus's ephemeris to a level where occultations can be accurately predicted at fixed sites. Moreover, only large telescopes will be able to observe occultations of the fainter candidates, and it may be necessary to plan observations of several appulse events to ensure that at least one actual occultation will be observed. Potential observers should contact the authors for refined predictions.

4. CONCLUSIONS

This paper presents accurate astrometry for 98,602 stars ($7.0 < V < 17.7$), whose positions have been searched for possible occultations by the Centaur 5145 Pholus in 1999–2005. Pholus is most likely a KBO that has been recently perturbed into the inner solar system, thereby making it an interesting object to observe because of its relative close-

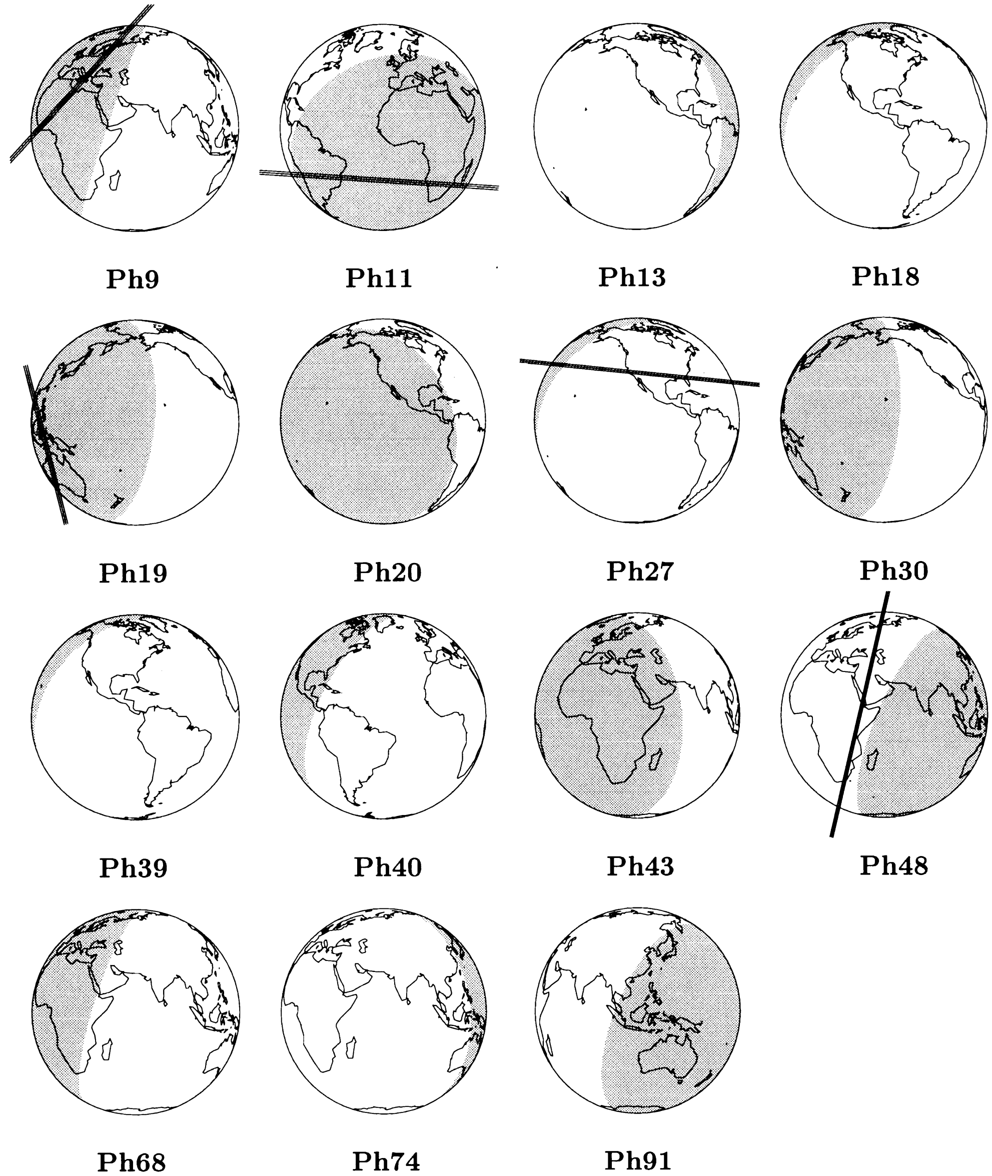

FIG. 6.—Maps of Earth as viewed from Pholus at the midtime of each potential occultation for the brightest occultation stars in Table 3 that are 40° or more from the Sun at appulse time. The shaded region of each globe represents that portion of Earth for which the Sun is more than 12° below the local horizon. Nominal occultation tracks for Pholus that cross Earth are shown with widths equal to ± 1 Pholus radius. Because of uncertainties in the current ephemeris for Pholus, these tracks are subject to considerable error and are intended to be only suggestive. In fact, tracks currently off Earth could move onto its surface with an improved ephemeris. For those globes with no shadow paths plotted, one can establish the orientation of the path from the position angle of Pholus at the time of closest approach given in Table 3.

ness. Among these stars, 100 are identified as potential occultation candidates and are listed in Table 3, and finder charts and visibility zones are given for the brighter ones, respectively, in Figures 5 and 6. Many of the occultation candidates are faint ($V > 15.0$) and, as a result, difficult to observe with portable telescopes. The best candidates in terms of apparent magnitude ($V < 14.0$) and minimum separations are Ph9, Ph11, Ph27, Ph48, and Ph78. Because of the small angular size of Pholus (radius ~ 10 mas), the width of its occultation shadow path across Earth will be very narrow, and consequently, a good prediction will require extremely good astrometry for updating its ephemeris and for any potential occultation star. Unfortunately, the current ephemeris for Pholus is not known very accurately, but it can be improved with new observations. This can be achieved with CCD observations of Pholus reduced with ACT reference stars. If fainter reference stars are needed, the accurate positions for the 98,602 stars computed in this paper can be used. Future observations of Pholus are planned, and updated predictions will be made available via the World Wide Web.[3] As a particular occultation draws near, its prediction can be significantly improved with last-minute astrometry, wherein both Pholus and the candidate occultation star are imaged on the same CCD frame using a large-aperture telescope and many frames are taken just prior to the event. Even with that, it might take several appulses before a successful occultation is observed.

Because of the ACT star catalog, positions of both stars and solar system objects can be determined now with great accuracy by using differential reductions. In particular,

[3] At http://occult.mit.edu.

identifying and predicting occultation events can be done now with much greater certainty. This paper discussed the case for 5145 Pholus, and in the future, other identifications and predictions will be made for other objects (e.g., Pluto/Charon, Chiron, and Triton).

We would like to thank the scientific staff at the US Naval Observatory (Flagstaff Station) for assisting in the taking of the observations presented in this paper, and this work was supported in part by NASA grant NAG 5-3940 (at MIT). Moreover, we would like to acknowledge the use of the Digitized Sky Survey, which was used to produce the finder charts presented in this paper. The survey was produced at the Space Telescope Science Institute under US government grant NAG W-2166 and is available to users through the Multimission Archive at STScI.

REFERENCES

Asher, D. J., & Steel, D. I. 1993, MNRAS, 263, 179
Binzel, R. P. 1992, Icarus, 99, 238
Bus, S. J., et al. 1996, Icarus, 123, 478
Campins, H., Telesco, C. M., Osip, D. J., Rieke, G. H., Rieke, M. J., & Schulz, B. 1994, AJ, 108, 2318
Elliot, J. L., et al. 1995, Nature, 373, 46
Green, R. M. 1985, Spherical Astronomy (Cambridge: Cambridge Univ. Press)
Henden, A. A., & Stone, R. C. 1998, AJ, 115, 296
Høg, E. 1997, in *Hipparcos* Venice '97, ed. B. Battrick (ESA SP-402) (Noordwijk: ESA), 25
Hoffmann, M., Fink, U., Grundy, W. M., & Hicks, M. 1993, J. Geophys. Res., 98, 7403
Johnston, K. J., et al. 1995, AJ, 110, 880
Levison, H. F., & Duncan, M. J. 1997, Icarus, 127, 13
Luu, J. X., & Jewitt, D. C. 1990, AJ, 100, 913
Ma, C., et al. 1998, AJ, 116, 516
McDonald, S. W., & Elliot, J. L. 1995, AJ, 109, 1352
———. 1996, AJ, 112, 788
Meech, K. J., & Belton, M. J. S. 1990, AJ, 100, 1323
Person, M. J., Bus, S. J., Wasserman, L. H., & Elliot, J. L. 1996, AJ, 112, 1683
Smart, W. M. 1977, Textbook on Spherical Astronomy (6th ed.; Cambridge: Cambridge Univ. Press)
Stone, R. C., Monet, D. G., Monet, A. K. B., Walker, R. L., Ables, H. D., Bird, A. R., & Harris, F. H. 1996, AJ, 111, 1721
Urban, S. E., Corbin, T. E., & Wycoff, G. L. 1998, AJ, 115, 2161
Weintraub, D. A., Tegler, S. C., & Romanishin, W. 1997, Icarus, 128, 456
Wilson, P. D., Sagan, C., & Thompson, W. R. 1994, Icarus, 107, 288